THE DESIGN OF SKEW GEARS FROM THE GEOMETRIC POINT OF VIEW

Hellmuth Stachel

Vienna University of Technology (AUSTRIA), stachel@dmg.tuwien.ac.at

Abstract

The modeling of the tooth flanks of gears with skew axes still represents a challenge to geometers. The problem is to attach to each wheel a surface such that, during uniform rotations of the two wheels, these surfaces remain in contact at a single point or along a line. We focus on two possibilities for designing simultaneously a pair of conjugate flanks. In both cases we present new proofs and report about new developments.

The first possibility dates back to Jack Phillips in 2003. He proved that helical developables serve as conjugate tooth flanks with point contact. Moreover, these types of flanks sustain errors upon assembly. There is even a case with permanent line contact, similar to helical involute gears with parallel axes. As a clarification of Phillips's achievements, particular attention is necessary when the transmission changes from front-to-front to back-to-back.

The second solution dates back to Martin Disteli in 1911. Based on the spatial Camus's Theorem, we obtain pairs of skew ruled surfaces which permanently are in contact along a straight line. As an example, we present spatial cycloidal gears and give an outlook to generalizations.

Keywords: Skew gears, cylindroid, involute gearing, cycloid gearing, Camus's Theorem, dual vectors.

1 INTRODUCTION

Designing a gear pair means obtaining a given transmission of the rotations from a driving or input wheel Σ_2 to a driven or output wheel Σ_3 by a pair of tooth flanks which are sliding on each other. We address this by focusing on general principles from the geometrical point of view, i.e., without paying attention to all deviations that real gear pairs undergo. To begin with, we recall a very few results on planar gearing, where the wheels' axes are supposed to be parallel, and we quote Phillips's version of the spatial Law of Gearing.

1.1 Involute spur gears

Conventional *involute spur gears* are regarded as superior in planar gearing. For this type of gearing, which was invented by L. Euler (1765), the tooth profiles c_2, c_3 are *circular involutes*, i.e., their evolutes are circles b_2 and b_3 called *base circles*. This type of gears is characterized by the condition that the common normal n_C to the profiles c_2 and c_3 at their contact point C remains fixed in the gear box Σ_1, which means that with respect to (w.r.t., for short) Σ_1 the meshing point C runs along a line.

For involute spur gears the helical tooth flanks are *helical developables*, also known as *helical involutes*. These developables $\mathcal{F}$ are swept out by the tangents of a helix *s*. The right cylinder $\mathcal{B}$ passing through *s* is called *base cylinder* and contains the base circle *b* of the involute spur gear (Fig. 1, left). Helical developables consist of two sheets which meet along the helix *s* called *cuspidal edge*. The *lower sheet* has its convex side pointing upwards w.r.t. the direction of the axis *a*, the convex side of the *upper sheet* points downwards (Fig. 1, right). A helical developable is uniquely defined, up to rigid motions, by the radius of the base cylinder and the pitch of the generating helical motion.

The surface normals of a helical developable $\mathcal{F}$ along any generator *g* are mutually parallel. The congruence of normals consists of lines which enclose a constant angle with the axis and contact the base cylinder. In the case of a left-handed developable the normals are right-twisted w.r.t. the axis. Along each generator *g* there exists an osculating cone with an axis g^* lying on the base cylinder and with its apex at the *cuspidal point* C^* of *g*, i.e., its contact point with the cuspidal edge *s* (Figs. 1, left, and 6).

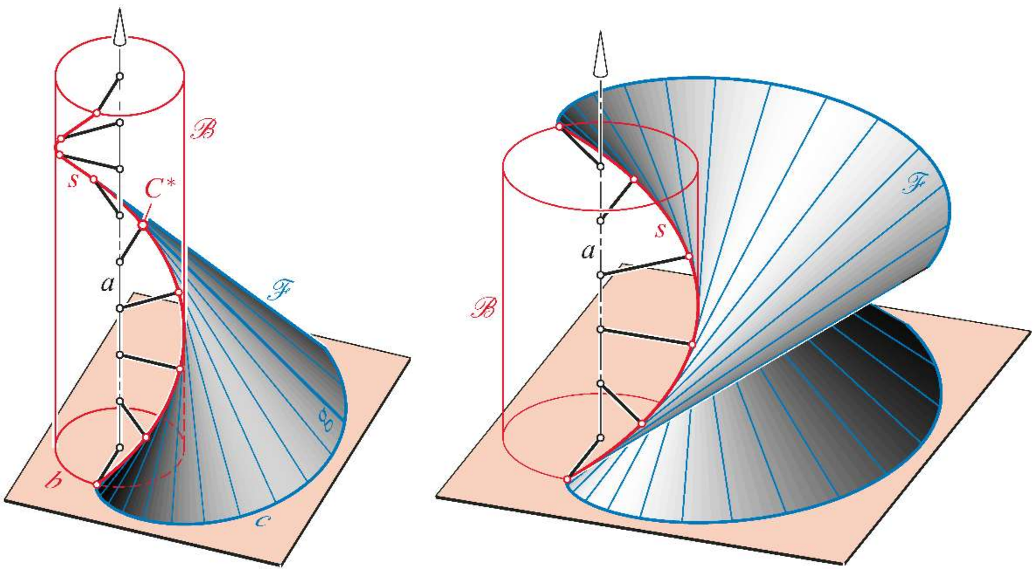

Fig. 1. Helical developable $\mathscr{F}$. Left: the lower sheet of $\mathscr{F}$ with the involute c of the circle b as cross section. Right: the two sheets of $\mathscr{F}$ meet on the cuspidal edge s, a helix on the base cylinder $\mathscr{B}$.

1.2 Camus's principle in the plane

The following theorem is attributed to C.É.L. Camus (1733), but most probably it dates back to Ph. de La Hire (1674) or Olaf Rømer (note [3]). It turns out that Camus's Theorem provides the most general principle of gearing, i.e., each pair of conjugate tooth profiles can be defined this way.[1]

Theorem 1 (Camus's Theorem). *If an auxiliary curve p_4 rolls on the pitch circles p_2 and p_3, then any point C attached to p_4 traces conjugate profiles c_2 and c_3, respectively.*

We rephrase this theorem by introducing an additional frame Σ_4, where the auxiliary curve p_4 is attached to. Let us assume that, simultaneously with the two rotating wheels Σ_2 and Σ_3 the *auxiliary frame* Σ_4 moves w.r.t. the gear box Σ_1 in such a way that $p_4 \subset \Sigma_4$ rolls on p_2 and p_3 and all mutual contacts take place at the pitch point $I_{42} = I_{43} = I_{32}$ fixed in Σ_1. If C is any point attached to Σ_4 and different from I_{32}, then the trajectories c_2 and c_3 of C under the relative motions Σ_4/Σ_2 and Σ_4/Σ_3, respectively, are in contact at C, since the respective path normals pass through the common pitch point $I_{42} = I_{43} = I_{32}$. Hence, $c_2 \subset \Sigma_2$ and $c_3 \subset \Sigma_3$ satisfy the planar Law of Gearing.

As an extension of Camus's classical result, not only the trajectories of points attached to Σ_4, but also the envelopes of curves attached to Σ_4 under the motions Σ_4/Σ_2 and Σ_4/Σ_3 are conjugate profiles.

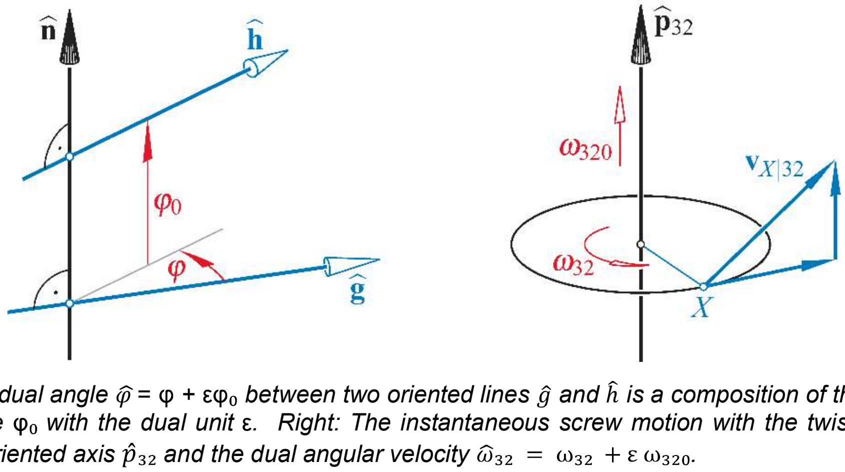

Fig. 2. Left: The dual angle $\widehat{\varphi} = \varphi + \varepsilon\varphi_0$ between two oriented lines $\hat{g}$ and $\hat{h}$ is a composition of the signed angle φ and the distance φ_0 with the dual unit ε. Right: The instantaneous screw motion with the twist $\hat{q}_{32} = \widehat{\omega}_{32}\widehat{p}_{32}$ is defined by the oriented axis $\hat{p}_{32}$ and the dual angular velocity $\widehat{\omega}_{32} = \omega_{32} + \varepsilon\,\omega_{320}$.

[1] To be precise, all profiles except their points which are located on the tangent to the pitch circles at the common pitch point.

1.3 Basics of spatial gearing

From now on the axes $\hat{p}_{21}$ and $\hat{p}_{31}$ of the two wheels are supposed to be skew. For the mathematical description, dual vectors are an adequate tool to represent oriented lines in space as well as instant screw motions (twists). For the sake of brevity, we skip the introduction into the dual vector calculus and refer only to the literature, e.g., to [8, 2]. At a few places below we will apply this tool. Therefore, we use the usual symbols for dual vectors and numbers as the labels of oriented lines, twists, dual angles, and dual angular velocities (note Fig. 2).

Instead of the pitch circles in the plane, we have in spatial gearing two hyperboloids as the axodes of the relative motion Σ_3/Σ_2 between the two wheels which rotate with the velocities ω_{21} and ω_{31} about the respective axes. The axodes are in contact along the instant screw axis $\hat{\boldsymbol{p}}_{32}$ called ISA, in short.

Without going into detail, we recall from [6], Chapter 2:

Theorem 2 (Law of Gearing, spatial version). *For gears with skew axes $\hat{p}_{21}$ and $\hat{p}_{31}$, the point C is a meshing point of conjugate tooth flanks $\mathcal{F}_2$, $\mathcal{F}_3$ if and only if the common surface normal n_C to the flanks at C encloses dual angles $\hat{\beta}_2, \hat{\beta}_3$ with the axes $\hat{p}_{21}$ and $\hat{p}_{31}$ (see Fig. 3) such that* [2]

$$\frac{\beta_{20}\ \sin\beta_2}{\beta_{30}\ \sin\beta_3} = \frac{\omega_{31}}{\omega_{21}}\,.$$

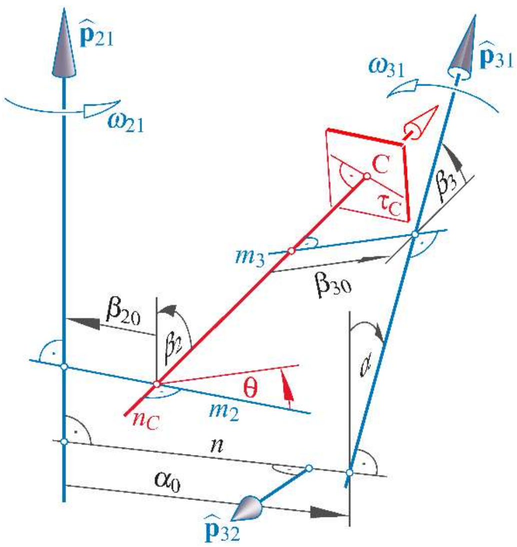

Fig. 3. Law of Gearing for skew gears.

2 PHILLIPS'S SPATIAL INVOLUTE GEARS

In 2003 Jack Phillips published a book [6] where he proved that helical involutes provide a uniform transmission not only for wheels with parallel axes but also for those with skew shafts. Moreover, as well as in the planar case, there is no transmission error in the case of misplacement. In the following, we present some basic results of this type of gearing, but we also focus on one inherent problem which hasn't been extensively discussed in [6] and in the related literature so far.

2.1 The role of helical developables

According to Phillips's definition, *spatial involute gears* are defined by the condition that during the mesh each meshing point *C* runs w.r.t. the gear box Σ_1 along its meshing normal n_C. According to the Law of Spatial Gearing (Theorem 2), the contact normal n_C at a single meshing point *C* outside ISA is sufficient

[2] The following formula is equivalent to the statement that n_C belongs to the linear line complex of path normals of the relative motion Σ_3/Σ_2 with the twist $\hat{q}_{32} = \omega_{31}\hat{p}_{31} - \omega_{21}\hat{p}_{21}$.

to determine the transmission ratio of a given spatial gearing. Therefore, Phillips's condition for a fixed meshing normal yields gears for a uniform transmission.

How can we find appropriate tooth flanks?

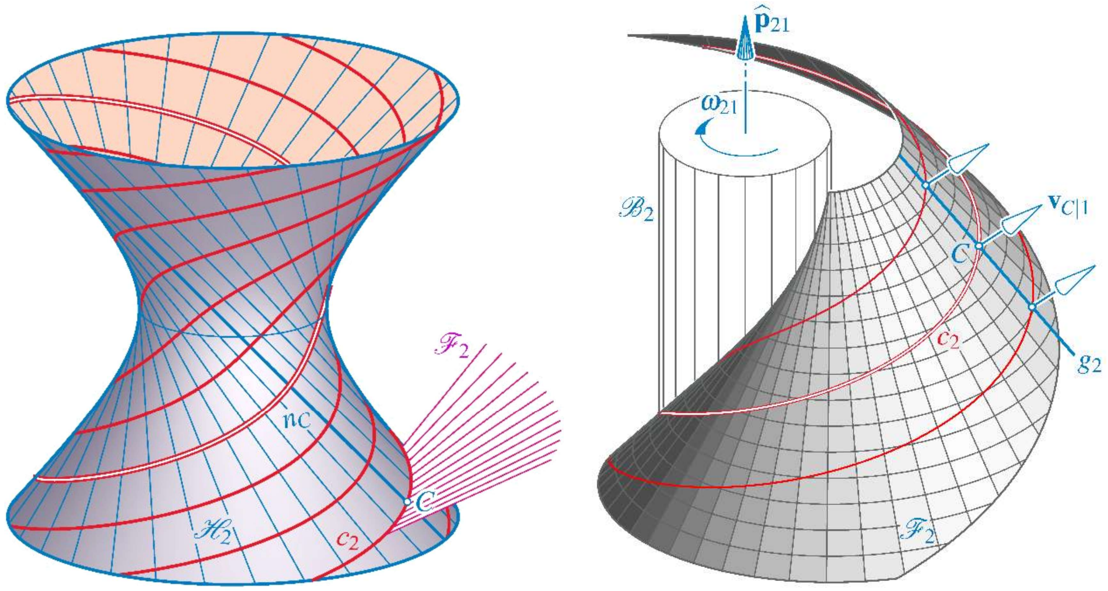

Fig. 4. The slip tracks are orthogonal trajectories of one regulus of the hyperboloid $\mathcal{H}_2$. Left: The rulings of $\mathcal{H}_2$ are normal lines of the helical developable $\mathcal{F}_2$ along the slip track c_2. Right: Lower sheet of the helical developable $\mathcal{F}_2$ with possible slip tracks.

During the mesh, the wheel Σ_2 rotates w.r.t. Σ_1 about the axis $\hat{p}_{21}$ with the angular velocity ω_{21}, while the contact point C runs along the fixed line n_C. On the other hand, w.r.t. Σ_2, point C traces on the tooth flank $\mathcal{F}_2$ a curve c_2 called *slip track* in [6]. At each point of c_2 the pose of n_C is orthogonal to $\mathcal{F}_2$ and therefore also orthogonal to $c_2 \subset \mathcal{F}_2$.

The movement of C against Σ_2 along c_2 is the composition C's movement along n_C w.r.t. Σ_1 and the inverse motion Σ_1/Σ_2 which is the rotation about $\hat{p}_{21}$ with the angular velocity $-\omega_{21}$. During this rotation the line n_C sweeps out a one-sheeted hyperboloid of revolution $\mathcal{H}_2$ in Σ_2. The trace c_2 of the contact point C w.r.t. Σ_2 belongs to this hyperboloid and is an orthogonal trajectory of one family of generators on $\mathcal{H}_2$. In Fig. 4, left, such orthogonal trajectories c_2 are depicted; they have the shape of a 'bed spring curve'.

Each surface that passes through c_2 with tangent planes τ_C orthogonal to the corresponding generators $n_C \subset \mathcal{H}_2$ serves as a tooth flank $\mathcal{F}_2$ for a single point contact on a contact normal n_C, which remains fixed in the machine frame Σ_1. The simplest choice is the envelope of these planes τ_C w.r.t. Σ_2.

Theorem 3. *Let skew gears with a uniform transmission from Σ_2 to Σ_3 be given. If the respective tooth flanks $\mathcal{F}_2$ and $\mathcal{F}_3$ are in permanent single point contact such that the meshing normal n_C remains fixed in the gear box Σ_1, then the envelopes of the common tangent planes τ_C at the meshing points C w.r.t. Σ_2 and Σ_3 are helical developables. For a constant driving velocity ω_{21} the meshing point C runs w.r.t. Σ_1 with a constant velocity along n_C.*

Proof. The movement of C w.r.t. Σ_1 along the fixed line n_C is the composition of a rotation about $\hat{p}_{21}$ and a movement along the slip track c_2. Therefore, the velocity vector $\boldsymbol{v}_{C|1}$ of C along n_C is the sum of the velocity vector $\boldsymbol{v}_{C|21}$ caused by the rotation of Σ_2 about $\hat{p}_{21}$, and a tangent vector $\boldsymbol{v}_{C|2}$ to c_2 orthogonal to n_C and $\boldsymbol{v}_{C|1}$. Fig. 5 shows this decomposition in the top view, i.e., after projection in direction of $\hat{p}_{21}$, and in a front view, obtained by orthogonal projection into a plane parallel to $\hat{p}_{21}$ and n_C.

The rotation about $\hat{p}_{21}$ assigns to *C* the velocity with

$$||\boldsymbol{v}_{C|21}|| = ||\boldsymbol{v}_{C|21}{}'|| = \omega_{21}\ \mathrm{dist}(C'\ \hat{p}_{21}{}') = \frac{|\omega_{21}\beta_{20}|}{|\cos\gamma|}\ .$$

This yields for the front view $||\boldsymbol{v}_{C|21}{}''|| = |\omega_{21}\beta_{20}|$. In other words, for each choice of *C* on the line n_C the front view $\boldsymbol{v}_{C|21}{}''$ has the same length, provided that ω_{21} is constant. Therefore, the velocity $v_{C|1}$ of *C* along n_C is constant, too, namely (Fig. 5) $v_{C|1} = ||\boldsymbol{v}_{C|1}|| = |\omega_{21}\beta_{20}\sin\beta_2|$ with β_2 as the slope angle of τ_C.

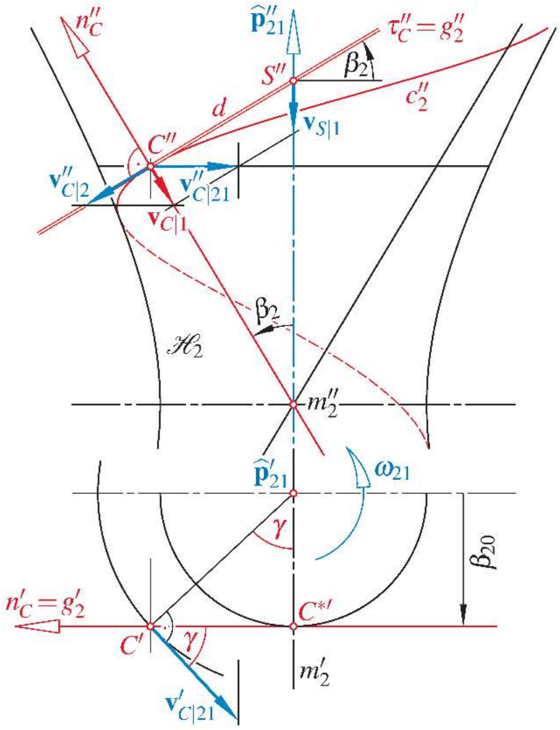

Fig. 5. Velocity analysis of the meshing point C, shown in the front view (above) and the top view (bottom).

The common tangent plane τ_C to the tooth flanks at the meshing point *C* intersects the axis $\hat{p}_{21}$ at a point *S*, which moves along the axis with the constant velocity $|v_{S|1}| = ||\boldsymbol{v}_{C|1}||/\cos\beta_2 = |\ \omega_{21}\beta_{20}\tan\beta_2|$. Hence, τ_C envelops a helical developable with the axis $\hat{p}_{21}$ and the pitch $h_2 = \beta_{20}\tan\beta_2$. This confirms that each orthogonal trajectory of one regulus on a one-sheeted hyperboloid belongs also to a helical developable (see Fig. 4, right, and note [9], p. 438, or [4], p. 408).[3] The line g_2 in τ_C with the top view g_2' coinciding with n_C' (see Fig. 5) is a generator of the envelope. ■

Conversely, let $\mathcal{F}_2$ be the helical developable with axis $\hat{p}_{21}$ and with the cuspidal edge s_2 on the base cylinder with radius β_{20} and pitch h_2. A rotation of $\mathcal{F}_2$ about its axis $\hat{p}_{21}$ through the angle φ_{21} together with a translation along $\hat{p}_{21}$ by $\varphi_{21}h_2$ transforms $\mathcal{F}_2$ into itself. Hence, a pure rotation through φ_{21} has the same effect on $\mathcal{F}_2$ (as a whole) like a translation by $-\varphi_{21}h_2$. This translation sends a generator g_2 of $\mathcal{F}_2$ with its tangent plane into a parallel line and plane at the distance $-\varphi_{21}h_2\cos\beta_2$ where $\tan\beta_2 = h_2\beta_{20}$ is the slope of s_2 (see Fig. 5). Consequently, the rotation about its axis through φ_{21} transforms a helical

[3] The top view of c_2 is the trajectory of a point under an involute motion where a line as the moving pitch curve rolls on a circle. For points *C* of c_2 on the generator g_2 of $\mathcal{F}_2$, the distance *d* to the cuspidal point C^* of g_2 increases with the constant signed velocity $v_S\sin\beta_2$ (note Fig. 5). Therefore, two different slip tracks cut the generators of $\mathcal{F}_2$ in pieces of equal lengths.

involute into an offset[4] at the distance $-\varphi_{21}\beta_{20}$ sin β_2, and in accordance with our previous result for $||\boldsymbol{v}_{C|1}'||$ we obtain for the signed velocity in the direction of n_C

$$v_{C|1} = -\,\omega_{21}\,\beta_{20}\sin\beta_2 \tag{1}$$

where $\pi/2 + \hat{\beta}_2$ is the dual angle between g_2 and the axis $\hat{p}_{21}$ (see also Fig. 4, right).

When $\mathcal{F}_2$ rotates with the angular velocity ω_{21}, then the generator $g_2 \subset \mathcal{F}_2$ through the meshing point C remains parallel to itself and moves together with the tangent plane τ_C in the direction of $n_C \perp \tau_C$ with the velocity $v_{C|1}$ given in (1). Suppose that a second helical developable $\mathcal{F}_3$ is in contact with $\mathcal{F}_2$ at the point C with the common tangent plane τ_C. If the two surfaces rotate about their respective axes $\hat{p}_{21}$, $\hat{p}_{31}$ with angular velocities ω_{21}, ω_{31} such that

$$\frac{\omega_{31}}{\omega_{21}} = \frac{\beta_{20}\sin\beta_2}{\beta_{30}\sin\beta_3},$$

then in both cases the point C together with the common tangent plane τ_C is shifted orthogonally to τ_C with the same velocity. This means that the contact between the two surfaces is preserved, wheresoever the axes of the two wheels have been located. We realize that the condition above is equivalent to the Law of Gearing in Theorem 2.

Theorem 4 (Jack Phillips's spatial involute gearing). *Whenever two helical developables $\mathcal{F}_2$ and $\mathcal{F}_3$ are in contact at a single point C and rotate about their axes $\hat{p}_{21}$, $\hat{p}_{31}$ with respective velocities ω_{21}, ω_{31} such that the dual angles $\hat{\beta}_2, \hat{\beta}_3$ between any orientation of the contact normal n_C and the axes satisfy the Law of Gearing (Theorem 2, note Fig. 3), then the two surfaces remain in contact with a fixed contact normal n_C. Therefore, these surfaces serve as tooth flanks with single point contact for a uniform transmission from $\hat{p}_{21}$ to $\hat{p}_{31}$, and they sustain errors upon assembly.*

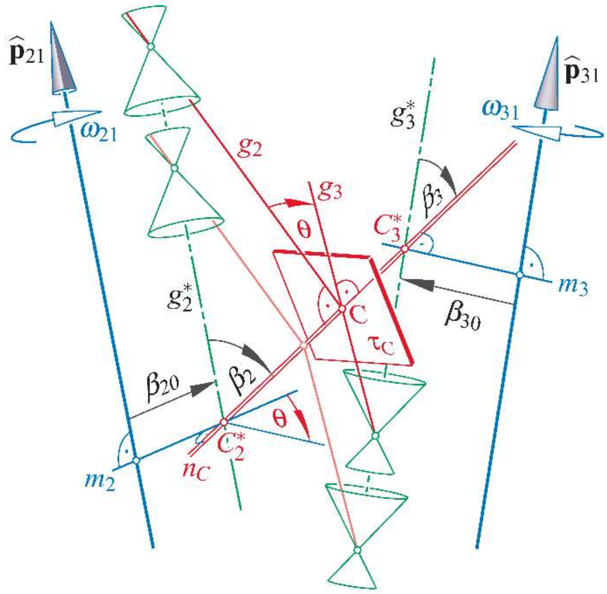

Fig. 6. At skew involute gearing the generators g_2, g_3 through the meshing point C enclose a constant angle θ, while they are translated within tangent planes to the respective base cylinders $\mathcal{B}_2$, $\mathcal{B}_3$. Simultaneously the osculating cones (green) along the generators g_2 and g_3 are translated along their axes $g_2^* \subset \mathcal{B}_2$ and $g_3^* \subset \mathcal{B}_3$.

Remark 1. Note that Theorem 4 includes the case of bevel gears and spur gears, the latter only in the case θ = 0. In [6], Chapter 7, involute gears are used for worm gears. A similar application is discussed in [10].

[4] This is the spatial counterpart to a similar property of circular involutes in the plane.

According to Fig. 5, the generator $g_2 \subset \mathcal{F}_2$ through the meshing point C spans with n_C a plane which contacts the base cylinder of $\mathcal{F}_2$. Consequently, g_2 is orthogonal to the common normal m_2 of $\hat{p}_{21}$ and n_C. Similarly, the plane connecting the generator $g_3 \subset \mathcal{F}_3$ through C with n_C contacts the base cylinder of $\mathcal{F}_3$ and is orthogonal to the common normal m_3 of $\hat{p}_{21}$ and n_C. Since the four lines g_2, g_3, m_2, and m_3 are orthogonal to n_C, we can conclude from $g_2 \perp m_2$ and $g_3 \perp m_3$ that the angles $\measuredangle\, m_2 m_3$ and $\measuredangle\, g_2 g_3$ are congruent. This confirms a result which was first stated in [7]:

Theorem 5. *At spatial involute gearing, the angle θ between the tooth flanks' generators g_2 and g_3 through the meshing point C remains constant during the mesh. This angle is congruent to the angle enclosed by the common perpendiculars m_2 and m_3 between the meshing* normal n_C *and the respective axes $\hat{p}_{21}$ and $\hat{p}_{31}$ (Fig. 6). In the particular case θ = 0 the flanks $\mathcal{F}_2$ and $\mathcal{F}_3$ are even in permanent contact along a line $g_2 = g_3$, the two axes $\hat{p}_{21}$, $\hat{p}_{31}$ and the fixed meshing normals n_C are parallel to a plane, and the base cylinders of $\mathcal{F}_2$ and $\mathcal{F}_3$ contact each other.*

Remark 2. The case θ = 0 is a spatial analogue of involute spur gears with vanishing pressure angle. These gears are not feasible due to the osculation between the conjugate involutes. By the way, the case θ = 0 with permanent line contact between the conjugate developable tooth flanks has been included, but not explicitly mentioned in 1922 by E. Stübler in [9], Satz I, where all spatial gears with developable tooth flanks and permanent line contact are characterized.

2.1 Conditions for a physical contact between the tooth flanks

While the meshing point C is running along n_C during the mesh, the generator g_2 varies on $\mathcal{F}_2$. However, w.r.t. the gear box Σ_1 the line g_2 remains in the plane through n_C and parallel to the axis $\hat{p}_{21}$. This plane contacts the base cylinder of $\mathcal{F}_2$ along the line g_2*, the locus of the respective cuspidal points C_2* of g_2 and common axis of the cones that osculate $\mathcal{F}_2$ along the moving line g_2 (Fig. 6).

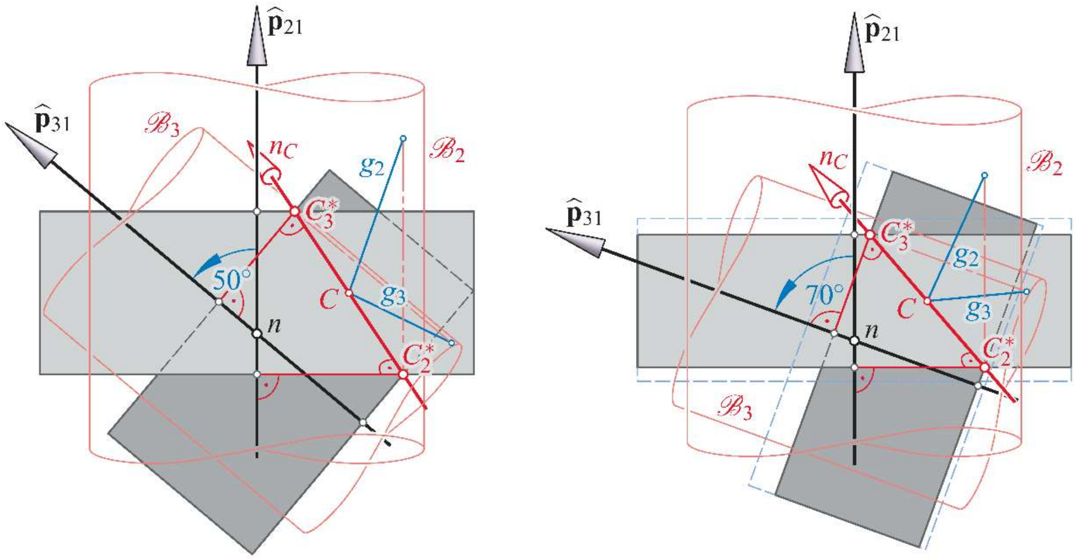

Fig. 7. Two mating involute gears schematically depicted in a view along the common normal n of the two axes $\hat{p}_{21}$ and $\hat{p}_{31}$. The crossing angle between the axes varies between α = $\measuredangle\, \hat{p}_{21}\hat{p}_{31}$ = 50° (left) and α = 70° (right). In both cases, the meshing normal n_C (red) is determined as a common tangent of the base cylinders $\mathcal{B}_2$ und $\mathcal{B}_3$. It contacts the cylinders at the respective extreme meshing points C_2 and C_3*.*

Similarly, the cuspidal points C_3* of the generators $g_3 \subset \mathcal{F}_3$ are located on the generator g_3* of the base cylinder of $\mathcal{F}_3$, and g_3* is the common axis of the osculating cones of $\mathcal{F}_3$ along the moving generator g_3 through the meshing point.

As long as the meshing point C lies between C_2* and C_3*, we have external gears and the convex sides of the developables $\mathcal{F}_2$ and $\mathcal{F}_3$ are meeting. Otherwise there is an undercut since the convex side of one developable meets the concave side of the other; the helical developables intersect each other in the neighbourhood of the contact point. The only exception with locally non-intersecting internal gears is possible for θ = 0.

Case θ ≠ 0: A feasible contact between $\mathcal{F}_2$ and $\mathcal{F}_3$ can only take place between the respective cross sections in planes passing through C_2* and C_3*. This terminates the mesh of the developables $\mathcal{F}_2$ and $\mathcal{F}_3$ without restricting the uniform transmission. We demonstrate this in an example:

Fig. 7 shows the schematic contours of two involute gears if seen along the common perpendicular *n* of the axes $\hat{p}_{21}$ and $\hat{p}_{31}$. The two pictures show the gears in two different meshing poses. While the distance α_0 between the axes remains the same, the crossing angle α varies between 50° and 70°.[5] The respective meshing normal n_C is determined as a common tangent of the respective base cylinders $\mathcal{B}_2$ und $\mathcal{B}_3$ and encloses given angles β_2 and β_3 with the axes. Moreover, depending on the given helical tooth flanks $\mathcal{F}_2$ and $\mathcal{F}_3$, the meshing normal must be respectively right-twisted or left-twisted to the axes. Apparently, the variation of the crossing angle α influences the extreme meshing points $C_2^* \in \mathcal{B}_2$ and $C_3^* \in \mathcal{B}_3$ as well as that of the extreme crossing sections, and moreover the addendum- and dedendum-hyperboloids (not depicted).

In order to obtain involute gears for the reversed rotation or the driving wheel, we exchange the upper and lower helical developables as tooth flanks.[6] This can be carried out by reflecting $\mathcal{F}_2$ and $\mathcal{F}_3$ simultaneously in the common normal *n* of the axes, called *center distance line*. This reflection does not change the base cylinders while their common tangent n_C is sent to the meshing normal $\overline{n}_C$ of the reflected surfaces $\overline{\mathcal{F}}_2$ and $\overline{\mathcal{F}}_3$ (Fig. 8, left [7]). The reflected extreme meshing points $\overline{C}_2$* and $\overline{C}_3$* indicate the terminating cross sections from the viewpoint of the reversed rotations. Consequently, involute gears can be used for rotations in both driving directions only if the common perpendicular *n* lies between the terminating cross sections of both wheels. However, this is necessary, but not sufficient, as Theorem 6 reveals.

Case θ = 0: As stated in Theorem 5, in this case the two base cylinders contact each other, i.e. $\alpha = \beta_2 + \beta_3$ and $\alpha_0 = \beta_{20} + \beta_{30}$ (see Fig. 8, right). The conjugate sheets of the tooth flanks contact along a line. This means that the meshing normal n_C is not unique but can be translated locally within the common tangent plane of the two base cylinders $\mathcal{B}_2$ and $\mathcal{B}_3$. It is still true that on each meshing normal n_C at all points *C* between the contact points C_2* and C_3* the convex side of $\mathcal{F}_2$ touches the convex side of $\mathcal{F}_3$ (Fig. 6).

This case is sensitive against misplacement. If there is any incorrectness, then instead of a line contact between the tooth flanks there will only be a single point contact.

In the summary below the term *interior of a wheel* stands for the space inside the addendum hyperboloid or cylinder and between the terminating cross sections.

Theorem 6. *Referring to the previous notation with n_C and $\overline{n}_C$ being symmetric w.r.t. the center distance line n, a pair of skew involute gears can transmit rotations in both directions with the same dual angles $\hat{\beta}_2, \hat{\beta}_3$ if and only if*

(i) The point of the meshing normals n_C and $\overline{n}_C$ in the interiors of the wheels lie between the terminating points C_2, C_3* and their mirrors $\overline{C}_2$*, $\overline{C}_3$*, respectively, and*

[5] The other data used in Fig. 7 are α_0 = 62.4 mm (= distance $\hat{p}_{21}\hat{p}_{31}$), $\beta_2 = \measuredangle\, \hat{p}_{21} n_C$ = 54.0°, β_{20} = 33.6 mm, $\beta_3 = \measuredangle\, \hat{p}_{31} n_C$ = 47.347°, β_{30} = 24.6 mm (compare with Fig. 3), θ = 114.27° (left) and θ = 84.58° (right), transmission ratio $\omega_{31} : \omega_{21}$ = -3 : 2. The upper sheet of $\mathcal{F}_2$ contacts the lower sheet of $\mathcal{F}_3$.

[6] Phillips mentions in [6] that for the backs of the teeth once more the principles of involute actions have to be applied. His book [6] shows pictures with flanks on one side (e.g., Fig. 4.11) and others with complete teeth (e.g., Figs. 5B.13 or 7.04). The latter indicate that the base cylinders and the angles β_2 and β_3 for both sides seem to be rather the same. In our study we restrict us only to this assumption and exchange upper and lower sheets of the developables.

[7] The dimensions of the example depicted in Fig. 8, left, are: $\alpha = \measuredangle\, \hat{p}_{21}\hat{p}_{31}$ = 62.0°, distance between the axes α_0 = 70.6 mm, $\beta_2 = \measuredangle\, \hat{p}_{21} n_C$ = 54.0°, β_{20} = 33.0 mm, $\beta_3 = \measuredangle\, \hat{p}_{31} n_C$ = 43.147°, β_{30} = 26.0 mm, θ = 94.21°, transmission ratio $\omega_{31} : \omega_{21}$ = -3 : 2. The upper sheet of $\mathcal{F}_2$ contacts the lower sheet of $\mathcal{F}_3$.

(ii) *the interiors of both wheels share a common segment on n_C as well as on $\overline{n}_C$. In the case* θ = 0 *one meshing normal n_C out of infinitely many is sufficient.*

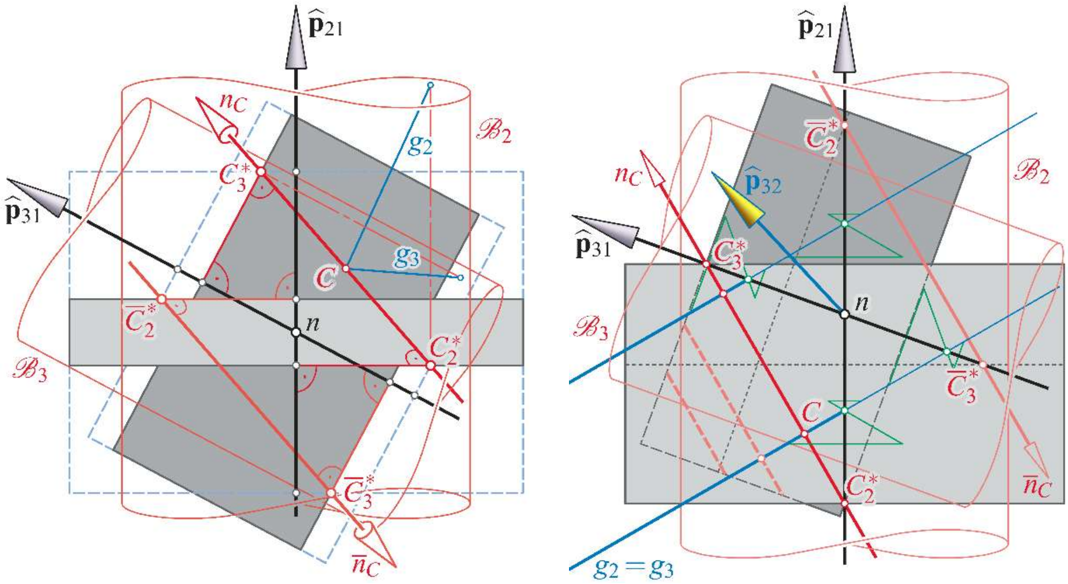

Fig. 8. Left: This view in direction of the common perpendicular n shows schematically the maximum dimensions of involute gears which can transmit rotations in both directions. Right: Case θ = 0 *with a permanent contact of the tooth flanks (indicated by the green osculating cones) along $g_2 = g_3$.*

3 THE SPATIAL CAMUS PRINCIPLE

Martin Disteli was the first who proved that a version of Camus's principle (Theorem 1) is even valid in space. It yields conjugate tooth flanks in the form of non-developable ruled surfaces which are in permanent contact along a straight line. Here we only lay out the basic ideas.

Let the motions of two gears be given, i.e., the rotations Σ_2/Σ_1, Σ_3/Σ_1 about fixed skew axes $\hat{p}_{21}$ and $\hat{p}_{31}$ with angular velocities ω_{21}, ω_{31}, respectively. Similar to the planar case we ask: is there an *auxiliary system* Σ_4 which can move in such a way that the motions Σ_4/Σ_2 and Σ_4/Σ_3 have twists with the same axis $\hat{p}_{32}$ and the same pitch $h_{32} = \omega_{320}/\omega_{32}$, as pertaining to the relative motion Σ_3/Σ_2 of the two gears?

This means in terms of dual vectors: Given the twists $\hat{q}_{21} = \omega_{21}\hat{p}_{21}$ and $\hat{q}_{31} = \omega_{31}\hat{p}_{31}$ with $\omega_{21}, \omega_{31} \in \mathbb{R}$ (note Fig. 2), we seek a system Σ_4 such that $\hat{p}_{42} = \hat{p}_{43} = \hat{p}_{32}$ and the dual velocities are proportional, i.e., there are factors $\lambda_2, \lambda_3 \in \mathbb{R}$ such that $\widehat{\omega}_{42} = \lambda_2\, \widehat{\omega}_{32}$, $\widehat{\omega}_{43} = \lambda_3\, \widehat{\omega}_{32}$ and consequently $\hat{q}_{42} = \lambda_2\, \hat{q}_{32}$ and $\hat{q}_{43} = \lambda_3\, \hat{q}_{32}$.

Upon recalling the spatial Aronhold-Kennedy Theorem we obtain $\hat{q}_{41} - \hat{q}_{21} = \lambda_2(\hat{q}_{31} - \hat{q}_{21})$ and $\hat{q}_{41} - \hat{q}_{31} = \lambda_3(\hat{q}_{31} - \hat{q}_{21})$, hence, $\lambda_2 - \lambda_3 = 1$ and

$$\hat{q}_{41} = \widehat{\omega}_{41}\hat{p}_{41} = \lambda_2\, \hat{q}_{31} + (1 - \lambda_2)\, \hat{q}_{21} = \lambda_2\, \omega_{31}\hat{p}_{31} + (1 - \lambda_2)\, \omega_{21}\hat{p}_{21}. \qquad (2)$$

The twist $\hat{q}_{41}$ is an affine combination of $\hat{q}_{21}$ and $\hat{q}_{31}$. This implies (see, e.g., [1]) that the instant axis $\hat{p}_{41}$ is located on Plücker's conoid $\mathfrak{C}$ (Fig. 9) defined by the given gear axes $\hat{p}_{21}$ and $\hat{p}_{31}$. Conversely, as long as $\hat{p}_{41}$ lies on $\mathfrak{C}$ and the dual velocity $\widehat{\omega}_{41}$ satisfies (2), Σ_4 serves as an auxiliary frame. For details, the reader is referred to [2].

Theorem 7 (Spatial Camus's Theorem). *Let two wheels Σ_2, Σ_3 with skew axes $\hat{p}_{21}$, $\hat{p}_{31}$ and angular velocities ω_{21}, ω_{31} be given. If an auxiliary system Σ_4 moves such that the instant screw axis $\hat{p}_{41}$ of Σ_4/Σ_1 is permanently located on Plücker's conoid $\mathfrak{C}$ and the twist $\hat{q}_{41}$ satisfies* (2)*, then for any line g attached to Σ_4 the ruled surfaces $\mathscr{F}_2$, $\mathscr{F}_3$ traced by g under the relative motions Σ_4/Σ_2 and Σ_4/Σ_3, respectively, are conjugate tooth flanks of Σ_3/Σ_2. During the mesh these flanks remain in contact along straight lines.*

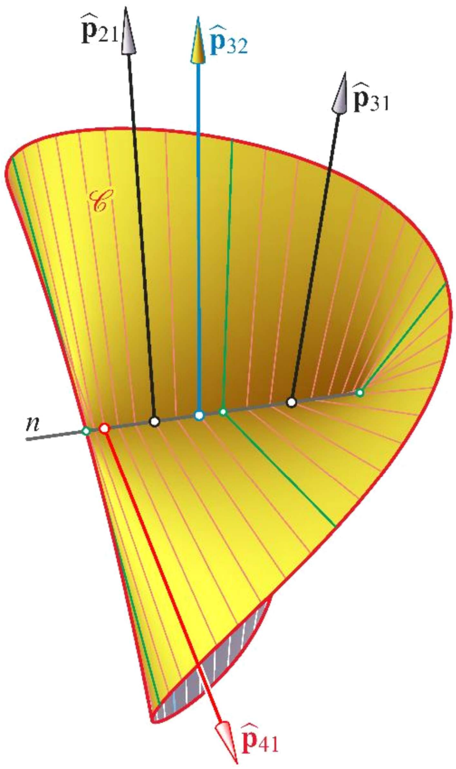

Fig. 9. Plücker conoid $\mathcal{C}$ with the wheels' axes $\hat{p}_{21}$ and $\hat{p}_{31}$, with the ISA $\hat{p}_{32}$ and the instant screw axis $\hat{p}_{41}$ of an auxiliary system Σ_4.

If a parametrized set of instant axes $\hat{p}_{41} \subset \mathcal{C}$ is given, then in general an integration is necessary to get an explicit representation of the auxiliary motion Σ_4/Σ_1. However, we can follow M. Disteli on his approach to generalizing the planar or spherical cycloidal gearing: We keep the axis $\hat{p}_{41}$ of Σ_4/Σ_1 fixed in the machine frame on $\mathcal{C}$ and simultaneously move Σ_2 with the twist $\hat{q}_{21}$ and Σ_3 with the twist $\hat{q}_{31}$. Furthermore, we move Σ_4 about the fixed axis $\hat{p}_{41}$ with the pitch $h_4 = \omega_{410}/\omega_{41}$ such that the relative axes $\hat{p}_{42}$ and $\hat{p}_{43}$ coincide permanently with $\hat{p}_{32}$. Under these motions the axodes of the relative motions Σ_3/Σ_2, Σ_4/Σ_2 and Σ_4/Σ_3 are obtained by applying the inverse motions, Σ_1/Σ_2, Σ_1/Σ_3 and Σ_1/Σ_4, to the ISA $\hat{p}_{32}$, which is fixed in Σ_1 (Fig. 10). Note that the spatial analogues of the circles p_2 and p_3 from Theorem 1 are one-sheeted hyperboloids, while the circle p_4 is replaced by a helical ruled surface, the trace of the ISA $\hat{p}_{32}$ under the helical motion Σ_4/Σ_1.

3.1 A generalization

The formal replacement of unit vectors of $\mathbb{R}^3$ by dual vectors allows to transfer theorems from spherical geometry to spatial geometry. This process, which sends points of the unit sphere to oriented lines in 3-space, is called *Principle of Transference* or *Dualization*. In this sense, the dualization of conjugate spherical tooth profiles yields ruled tooth flanks for skew gears. For the dualization of the Camus principle it is important to notice that the real coefficients in (2), namely λ_2 and $(1 - \lambda_2)$, are already known from the spherical analogue. Hence, there is a unique solution for the twists of the corresponding spatial auxiliary motion which leads to conjugate skew ruled tooth flanks.

We can generalize: For each auxiliary system Σ_4, chosen according to Theorem 7, the twists $\hat{q}_{42}$, $\hat{q}_{43}$ and $\hat{q}_{32}$ of the respective motions Σ_4/Σ_2, Σ_4/Σ_3 and Σ_3/Σ_2 are proportional over $\mathbb{R}$. Consequently, each space point C attached to Σ_4 has proportional tangent velocity vectors $\boldsymbol{v}_{C|42}$, $\boldsymbol{v}_{C|43}$, and $\boldsymbol{v}_{C|32}$. Hence, the tangent lines at C to the respective trajectories are identical. Therefore, we can replace the line g (which is strictly dual to a point on the unit sphere) by an arbitrary curve c through C and attach it to Σ_4. Then the surfaces $\mathscr{F}_2$, $\mathscr{F}_3$ swept out by c under Σ_4/Σ_2 and Σ_4/Σ_3 are conjugate tooth flanks, since at each point $C \in c$ the tangent plane to both flanks is spanned by the tangent lines to c and to the respective trajectory. This is true even when the path contacts *c* since in this case the contact point *C* is a singularity of $\mathcal{F}_2$ and $\mathcal{F}_3$.

Moreover, we can even replace the curve *c* by any surface S attached to the auxiliary system Σ_4. The conditions for being an enveloping point of S under Σ_4/Σ_2 and Σ_4/Σ are the same, namely, that the contact normal is included in the linear complex associated to the twists $\hat{q}_{42}$ and $\hat{q}_{43}$, which are real multiples of $\hat{q}_{32}$.

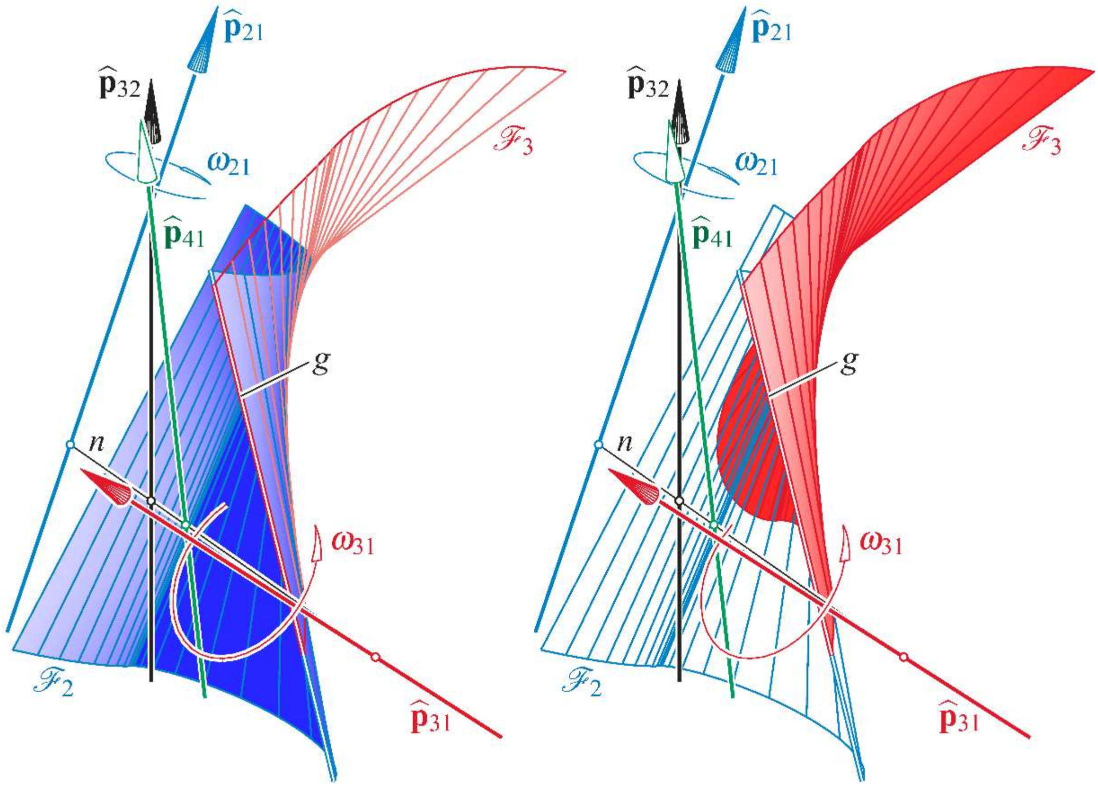

Fig. 10. Spatial cycloid gearing: The skew ruled surfaces $\mathcal{F}_2$ and $\mathcal{F}_3$ are in contact along the line g.

Theorem 8 (Spatial Camus's Principle, generalized). *Referring to Theorem 7, let Σ_4 be an appropriate auxiliary system. Then each curve c attached to Σ_4 traces conjugate tooth flanks* F_2, F_3 *under the relative motions Σ_4/Σ_2 and Σ_4/Σ_3, where the flanks are in permanent line contact along the respective poses of c under Σ_4/Σ_1. More general, each surface attached to Σ_4 envelopes conjugate tooth flanks under these motions.*

4 CONCLUSIONS

We discussed two methods for designing tooth flanks of spatial gears from the geometric point of view. Further studies will be necessary to optimize the design by checking the quality of the transmission. We are convinced that the spatial involute gearing is important in practice, in particular when the relative position of the wheels' axes, i.e., the crossing angle α and the shortest center distance α_0, need to be locally variable. In view of the spatial Camus principle, it remains open whether non-developable ruled surfaces with their hyperbolic surface points can be used as tooth flanks in practice. However, this method as well as its generalizations deserve interest as they provide flanks with a permanent line contact.

REFERENCES

[1] Disteli, M. (1911). *Über die Verzahnung der Hyperboloidräder mit geradlinigem Eingriff*. Z. Math. Phys. 59, pp. 244-298.

[2] Figliolini, G., Stachel, H., Angeles, J. (2007). *A new look at the Ball-Disteli diagram and its relevance to spatial gearing.* Mech. Mach. Theory 42(10), pp. 1362-1375.

[3] Figliolini, G., Stachel, H., Angeles, J. (2013). *On Martin Disteli's spatial cycloidal gearing*. Mech. Mach. Theory 60(1), pp. 73-89.

[4] Odehnal, B., Stachel, H., Glaeser, G. (2020). *The Universe of Quadrics*. Springer Spectrum, Berlin, Heidelberg.

[5] Pennock, G.R. (2023). *Jack Raymond Phillips (1923-2009)*. In Ceccarelli, M., Gasparetto, A. (eds). Distinguished Figures in Mechanism and Machine Science. History of Mechanism and Machine Science, vol. 41. Springer, Cham, pp. 137-161, https://doi.org/10.1007/978-3-031-18288-4_5

[6] Phillips, J. (2003). *General Spatial Involute Gearing.* Springer, Berlin, Heidelberg.

[7] Stachel, H. (2004). On *Jack Phillips' Spatial Involute Gearing*. Proceedings 11th International Conference on Geometry and Graphics, Guangzhou, P.R. China, pp. 43-48.

[8] Stachel, H. (2006). *Teaching Spatial Kinematics for Mechanical Engineering Students*. Proceedings 5th Aplimat, Bratislava/Slovak Republic (ISSN 80-967305-4-1), Part I, pp. 201-209.

[9] Stübler, E. (1922). *Über hyperboloidische Verzahnung*. Z. Angew. Math. Mech. 2, pp. 429-446.

[10] Xinxin Ye, Yonghong Chen, Binbin Lu, Wenjun Luo, Bingkui Chen (2022). *Study on a novel backlash-adjustable worm drive via the involute helical beveloid gear meshing with dual-lead involute cylindrical worm.* Mech. Mach. Theory 167, https://doi.org/10.1016/j.mechmachtheory.2021.104466